The Astrophysical Journal, 665:1159–1163, 2007 August 20

DIFFUSIVE COMPRESSION ACCELERATION OF ENERGETIC PARTICLES WITH AN APPLICATION TO SHOCK ACCELERATION NEAR INJECTION ENERGIES

Ming Zhang[1]
Department of Physics and Space Sciences, Florida Institute of Technology, Melbourne, FL 32901
Received 2006 December 14; accepted 2007 April 19

ABSTRACT

The behavior of energetic charged particles accelerated by a continuous plasma compression profile is explored in the framework of diffusion. At high enough energies, the accelerated particles have a power-law spectrum with a slope generally steeper than a shock spectrum with the same compression ratio. The spectral slope depends on the ratio of the diffusion coefficient to the product of the upstream plasma speed and the thickness of the compression region. In the limit of large diffusion, the spectrum becomes identical to that of diffusive shock acceleration, and when diffusion is small enough, it is consistent with adiabatic acceleration by a single passage through the compression region. For particles with a diffusion coefficient that increases with energy, the spectral shape of the accelerated particles changes from an adiabatic compressional acceleration spectrum at low energies to a shock spectrum at high energies. The flux level of the high-energy asymptotic shock spectrum is generally lower than that from a calculation with diffusive shock acceleration. When this result is applied to particles accelerated to high energies by shocks, the particle injection energy and efficiency can be determined once the energy dependence of the diffusion coefficient and the spectrum of the source particles are known. A threshold criterion for particle injection to shock acceleration can be set from the injection efficiency calculation.

Subject headings: acceleration of particles — cosmic rays — diffusion — shock waves

1. INTRODUCTION

Collisionless shock waves exist in various space plasma environments. They are believed to be able to accelerate charged particles to very high energies. For example, supernova shocks are a source of Galactic cosmic rays up to $\sim 10^{15}$ eV. In the solar system, the solar wind termination shock, shocks from coronal mass ejections (CMEs), interplanetary traveling shocks, and bow shocks ahead of planetary magnetospheres all have been observed to accelerate particles. Particle acceleration occurs every time a particle crosses the shock front. Scattering by the medium, both upstream and downstream, causes certain particles to cross the shock many times, and hence they achieve high energies. This is called diffusive shock acceleration and is regarded as one of the most important mechanisms in astrophysics. At the center of diffusive shock acceleration is the Parker transport equation for the isotropic part of the distribution function, $f(x, p, t)$, as a function of location x, particle momentum in the plasma frame p, and time t:

$$\frac{\partial f}{\partial t} = \frac{\partial}{\partial x}\left(\kappa \frac{\partial f}{\partial x}\right) - V\frac{\partial f}{\partial x} + \frac{p}{3}\frac{\partial V}{\partial x}\frac{\partial f}{\partial p}, \tag{1}$$

where κ is the diffusion coefficient on the x-axis along the shock normal and V is the speed of the background plasma. The rate at which particles gain momentum is $dp/dt = -\frac{1}{3}p\ \partial V/\partial x$, which is a δ-function at the shock front, representing acceleration every time a particle crosses it. Details of diffusive shock acceleration can be found in a review paper by Drury (1983).

There is a contradiction in the mathematics of diffusive shock acceleration theory when the diffusion coefficient approaches zero. The average time for a particle to be accelerated from p_0 to p is

$$t_{\rm acc} = \frac{3}{V_1 - V_2}\int_{p_0}^{p}\left(\frac{\kappa_1}{V_1} + \frac{\kappa_2}{V_2}\right)\frac{dp'}{p'} \tag{2}$$

(Drury 1983), where subscripts 1 and 2 denote upstream and downstream values of the variables. It takes no time to accelerate particles even to infinite momentum if the diffusion coefficient κ is set to zero, which is appropriate for either low-energy particles or a perpendicular shock. This situation obviously cannot happen in the physical world, for if there is no diffusion the particle just passes the shock once and its momentum is only boosted to $r^{1/3}$ times its initial value, where $r = n_2/n_1 = V_1/V_2$ is the shock compression ratio. This is one problem with the theory of diffusive shock acceleration at injection energies. Another problem with injection is that there is no clear standard to estimate the efficiency of and energy threshold for shock acceleration. There are a number of papers that have tried to address the injection problem, with various methods (see review by Scholer et al. [1999] and § 1 of Blasi et al. [2005]). A few papers argue that shocks can accelerate thermal particles without any trouble (e.g., Scholer & Kucharek 1999; Giacalone 2005), while others run into difficulty, so that additional preacceleration is required (e.g., Zank et al. 1996; Lee et al. 1996; Kallenbach et al. 2005).

One approach to the above difficulties is to use a mechanism other than diffusion, based on the argument that the diffusion equation (eq. [1]) will fail if the particle distribution in the plasma frame is too anisotropic (e.g., Malkov & Völk 1995), which can happen in certain situations. However, there are many observations that indicate diffusion may still be a good approximation because of the near-isotropic distribution of suprathermal particles (Gloeckler et al. 2001). Diffusion can happen to thermal particles too, as long as the Green-Kubo formula does not break down. Even at perpendicular shocks with a large pitch-angle anisotropy, the transport equation in the shock normal direction is still a diffusion equation, because the pitch angle drops out of the equation and becomes only a parameter. Efforts using the diffusion equation to tackle shock injection can also be found in other publications (e.g., Malkov 1997; Blasi et al. 2005).

In this paper, we try to maintain the use of the diffusion equation. This is particularly justified if we want to extend the validity

[1] Visitor, State Key Laboratory of Space Weather, 100080 Beijing, China.

of diffusive shock acceleration from high energies down to injection energies. We note that the above mathematical contradiction arises under two different limiting cases, depending on whether we consider the δ-function for $\partial V/\partial x$ first or zero diffusion coefficient first. In diffusive shock acceleration, we take a shock profile for V first, which implies that no matter how small the diffusion coefficient is, the shock is always thin enough to let particles go back upstream, and so we can obtain shock-type particle acceleration. For those who argue that diffusive shock acceleration should fail when the diffusion coefficient goes to zero, the diffusion term drops out of equation (1) first, before a shock velocity profile is put in, which implies that the shock is of finite thickness before the diffusion coefficient goes to zero. Therefore, the contradiction can be solved by prescribing a thickness for the shock. The comparison between the diffusion coefficient and shock thickness can then be set to different limiting cases. The study by Drury et al. (1982), with constant diffusion in a shock with continuously varying plasma speed, proved this remedy. Here we extend it to cases with a momentum-dependent diffusion coefficient. As the particle acceleration in this geometry is due to continuous compression in the transition layer, it has been called *diffusive compression acceleration*. Giacalone et al. (2002) used this mechanism to interpret particle observations in corotating interaction regions of solar wind streams. This type of acceleration can also be applied to other space environments, such as the magnetosphere (Zhang 2006).

2. MODEL AND RESULTS

For simplicity in dealing with the diffusion equation analytically, we take the following special one-dimensional profiles for the plasma speed and particle diffusion coefficient in the continuous compression layer:

$$V(x) = \begin{cases} -a_V x_1 = -V_1, & \text{for } x > x_1, \\ -a_V x, & \text{for } x_2 < x < x_1, \\ -a_V x_2 = -V_2, & \text{for } x < x_2; \end{cases} \tag{3}$$

$$\kappa(x) = \begin{cases} a_\kappa x_1^2 = \kappa_1, & \text{for } x > x_1, \\ a_\kappa x^2, & \text{for } x_2 < x < x_1, \\ a_\kappa x_2^2 = \kappa_2, & \text{for } x < x_2. \end{cases} \tag{4}$$

The compressional transition layer is $x_1 - x_2 = \Delta x_{\rm sh}$ thick, or $x_1 = \Delta x_{\rm sh} r/(r-1)$ and $x_2 = \Delta x_{\rm sh}/(r-1)$. In order to see the behavior of the particle acceleration with different degrees of diffusion, let us first consider a diffusion coefficient that is independent of particle momentum. The boundary condition is $f(x \rightarrow \infty, p, t) = p_0 \delta(p - p_0)$, which represents injection from a monoenergetic source. Solutions to the transport equation with another injection spectrum far upstream can be worked out from the Green's function for monoenergetic injection. Other choices of plasma speed and diffusion coefficient profiles, unless they take unreasonably odd forms, will affect the result in some quantitative details but will not change the conclusions of this paper. We only seek a steady state solution of equation (1), because we are mainly interested in particle acceleration at injection energies. In other words, there is enough time for the particle spectrum at these energies to have reached an equilibrium for further acceleration to higher energies.

With the above plasma speed and diffusion coefficient profiles, we can solve the transport equation analytically using a Laplace transform. The downstream particle distribution function ($x < x_2$) is uniform, with a spectrum

$$f(x < x_2, p, t) = \sum_{n=1}^{\infty} \text{Res}\, g(s_n) \left(\frac{p}{p_0}\right)^{-s_n}, \tag{5}$$

where Res $g(s_n)$ is the residue of function $g(s)$ at pole s_n:

$$g(s) = [\lambda_+(s) - \lambda_-(s)] \times \left\{ -\left[\frac{s}{3} + \lambda_-(s)\right] \left(\frac{V_1}{V_2}\right)^{\lambda_+(s)} + \left[\frac{s}{3} + \lambda_+(s)\right] \left(\frac{V_1}{V_2}\right)^{\lambda_-(s)} \right\}^{-1} \tag{6}$$

with

$$\lambda_{+,-}(s) = -\frac{1 + r_a}{2} \pm \sqrt{\frac{(1 + r_a)^2}{4} - \frac{r_a s}{3}}. \tag{7}$$

Here $r_a = a_\kappa/a_V = \kappa_2/V_2 x_2 = \kappa_1/V_1 x_1$. The function $g(s)$ has an infinite number of poles s_n, on the positive real axis only. The odd-numbered poles have positive residues, while even-numbered poles have negative residues. The solution for the accelerated particle spectrum (eq. [5]) is a summation of a series of power-law spectra. For large momenta, it is dominated by the power law with the lowest-slope index, s_1. A similar power-law spectrum was also observed in simulations by Giacalone et al. (2002). The higher poles have much larger s_n ($n = 2, \ldots$), meaning that they will only affect the spectrum at low momentum. Figure 1*a* shows the values of the first and second poles, s_1 and s_2, as a function of r_a. The compression ratio r is taken to be 4, appropriate for strong shocks. At large r_a, where the upstream diffusion scale κ_1/V_1 is much larger than the thickness of the compression layer, the lowest pole is consistent with the spectral index for shock acceleration, $s_{\rm sh} = 3r/(r-1)$. As r_a gets smaller, the spectrum of the lowest power-law index becomes steeper. This means that continuous compression is less effective at accelerating particles to high energies than a shock with the same compression ratio. On the other hand, since continuous compression is not necessarily limited to the maximum shock compression of 4, a spectral slope flatter than 4 but steeper than 3 is possible. The differences between the lowest spectral index and the higher ones become smaller with decreasing r_a, indicating that a summation to higher order poles becomes more necessary.

Figure 1*b* shows downstream particle spectra calculated using equation (5) for three different values of r_a. When r_a is larger than 10, the spectrum is almost identical to a shock acceleration spectrum. As r_a becomes smaller, the spectrum becomes more sharply peaked, with steeper slopes on both sides. In the limit $r_a \rightarrow 0$ the spectrum approaches $\delta(p - r^{1/3} p_0)$, what would result from a single convective passage through the compression region. Therefore, we can use the ratio r_a as a parameter to obtain different limiting cases for the acceleration. This result is consistent with that of Drury et al. (1982).

When talking about particle injection, one automatically thinks that particle transport should increase with particle momentum. In that case, we want to see how a momentum-dependent diffusion coefficient will affect the calculation. From the above result, we already know how the spectrum of accelerated particles should behave in the two extremes. Injection should be close to 100% if r_a is large enough at high momenta, and no injection will occur if r_a is too small. At intermediate r_a, the injection behavior becomes unclear. In this case, a full calculation with a momentum-dependent

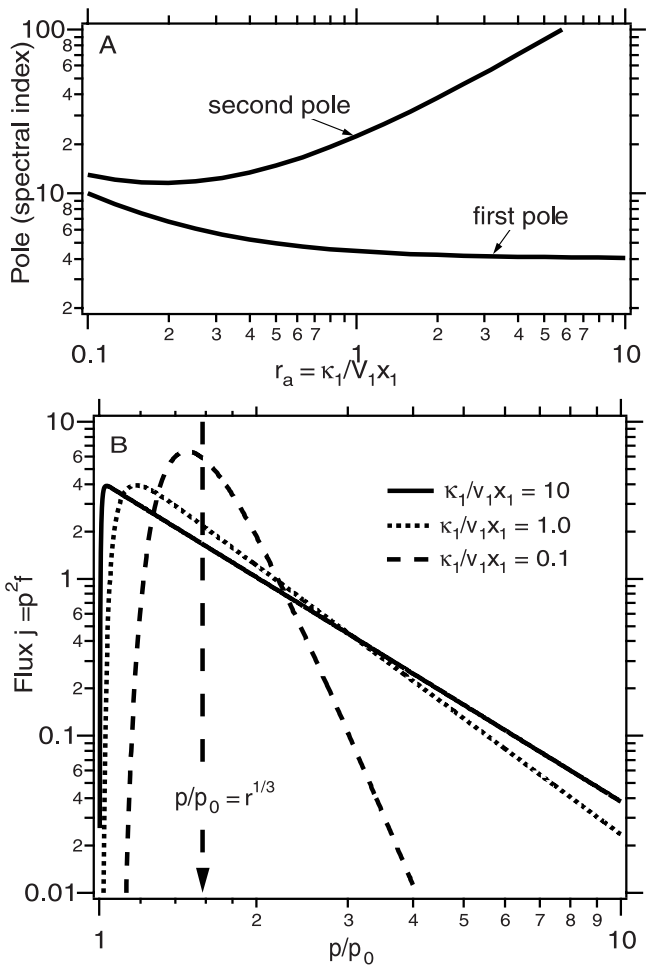

FIG. 1.—(*a*) First and second poles (spectral index) of $g(s)$ as a function of the ratio $r_a = \kappa_1/V_1x_1$. (*b*) Flux spectrum $j = p^2f$ as a function of particle momentum for three different values of κ_1/V_1x_1. The calculations are for a momentum-independent diffusion coefficient.

diffusion coefficient is needed. We solved the diffusion equation (eq. [1]) with a finite element method in MatLab. The spatial profiles of the parameters remain the same. The obtained result has been tested against the above analytical solution for a diffusion coefficient that is momentum independent.

Figure 2 shows a few calculation results for a diffusion coefficient proportional to p^2. Three different values of the diffusion coefficient at particle injection momentum $\kappa_1(p_0)$ were used. For the $\kappa_1(p_0)/V_1x_1 = 10$ case, the diffusion coefficient is already large enough at the injection momentum p_0, and the spectrum is consistent with shock acceleration. If $\kappa_1(p_0)$ decreases, the spectrum at low momentum is sharply peaked at the expected location of single-passage acceleration. Because κ increases with p, the diffusion coefficient becomes large enough beyond some value of the momentum that the spectrum approaches the same spectral slope as diffusive shock acceleration would produce (*dashed lines*). The flux level of the asymptotic shock spectrum at high momentum is generally lower than the level from the direct calculation using diffusive shock acceleration. The ratio of the two flux levels defines the efficiency of shock acceleration for particles injected at p_0, that is, the fraction of particles that attain a shock spectrum as viewed at high momentum.

Figure 3*a* shows the injection efficiency for shock acceleration, η, as a function of momentum when the particles are injected. For high enough momentum, the efficiency is 100%. The

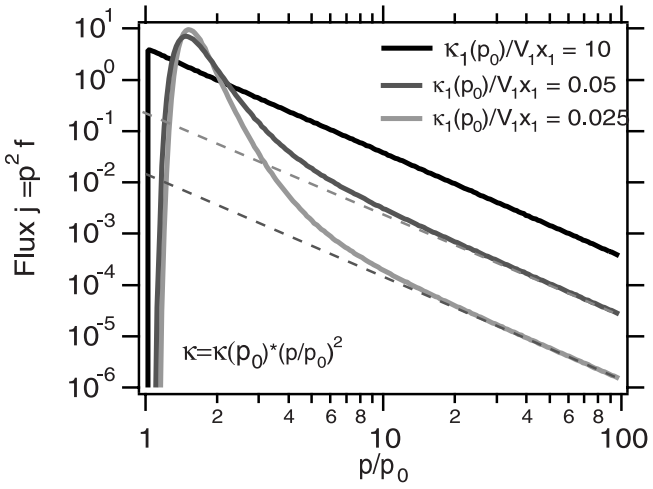

FIG. 2.—Downstream flux spectrum $j = p^2f$ as a function of particle momentum for three different values of κ_1/V_1x_1 at injection momentum p_0. The calculations are for a diffusion coefficient that is proportional to p^2. The dashed lines are the asymptotic spectra for high momenta.

injection efficiency decreases precipitously with p_0 once κ_1/V_1x_1 falls below 1. So, we set the threshold for fully efficient shock acceleration roughly at $\kappa_1/V_1x_1 = 1$. The sharpness of the decrease in efficiency depends on how fast the diffusion coefficient varies with momentum. Figure 3*a* displays the calculated injection efficiency for two profiles of diffusion-coefficient momentum dependence.

The momentum of the particles actually injected to shock acceleration also depends on the shape of the source particle spectrum,

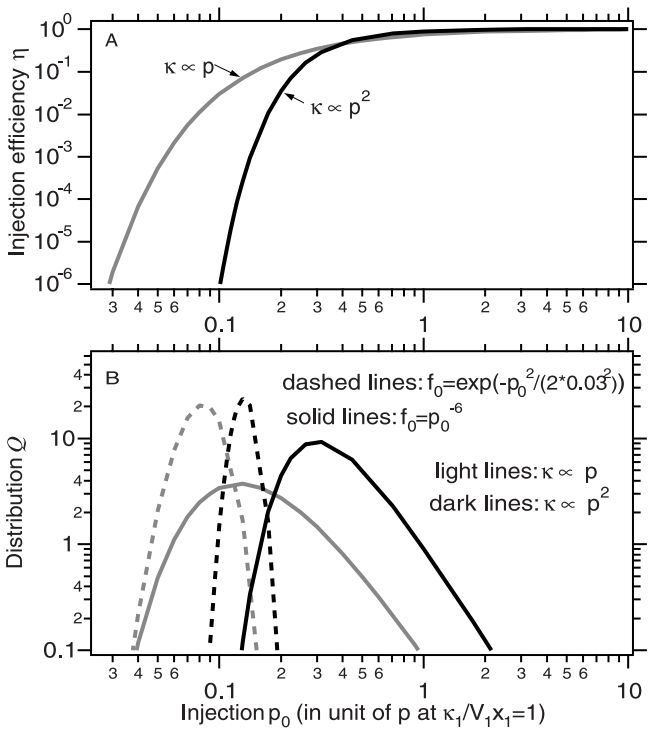

FIG. 3.—(*a*) Particle injection efficiency as a function of momentum upon injection for two different momentum dependences of the diffusion coefficient. (*b*) Normalized distributions of source particles that actually achieve shock acceleration. Two different types of source distribution, a power law and a Maxwellian, have been used in the calculation of the distribution of the source contribution.

TABLE 1
Typical Values of Proton Injection Speed with Nearly Full Efficiency for Shock Acceleration ($r = 4$ and $\eta_c = 6$)

Type	n (cm^{-3})	B (nT)	$\Delta x_{sh} = c/\omega_{pi}$ (km)	V_1 (km s^{-1})	$v_i^{(\parallel)}$ (km s^{-1})	$v_i^{(\perp)}$ (km s^{-1})
Supernova shock	1	0.3	227	5000	147	895
Termination shock	5×10^{-4}	0.02	10163	300	62	380
CME shock	10^6	5×10^4	0.227	1000	852	5180
Earth bow shock	5	5	101	400	113	690
Interplanetary shock (1 AU)	5	5	101	100	57	345
Interplanetary shock (10 AU)	0.05	0.2	1010	100	36	218

because the distribution function of accelerated particles at large enough momentum p is

$$f(x < x_2, p, t) = \int_0^p \eta(p_0)[f_0(p_0)/p_0]s_{sh}(p/p_0)^{-s_{sh}}dp_0, \quad (8)$$

where $f_0(p_0)$ is the distribution function of the source particles and the first s_{sh} comes from Res $g(s_1)$ at $\kappa_1/V_1x_1 \to \infty$. Then the distribution of injected particles contributing to shock acceleration is equal to $Q(p_0) = s_{sh}\eta(p_0)f_0(p_0)p_0^{s_{sh}-1}$. Figure 3*b* shows normalized curves of the source particle distribution as a function of injection momentum. Two different source spectra were used in the calculations. If the source spectrum is much softer than the shock acceleration spectrum, then the distribution of the injected source particles is sharply peaked at a fraction of $p_0 = 1$ (in units of the momentum value at which $\kappa_1/V_1x_1 = 1$). This means that most of the particles injected have low efficiencies for shock acceleration. For example, let us take $\kappa \propto p^2$. If the source particles have a p_0^{-6} power-law distribution function, the injected particles peak at $p_0 = 0.3$ and the injection efficiency is ~30%. But if the source particles have a Maxwellian distribution exp $[-p_0^2/(2 \times 0.03^2)]$, then the peak injection moves to $p_0 = 0.12$ and the injection efficiency is much lower, of order 10^{-4}. Note that neither the injection energy nor the injection efficiency at the peak contribution alone can determine the flux of accelerated particles. If the source contribution distribution $Q(p_0)$ is sharply peaked at p_m, the value $[2\pi Q^3(p_m)/Q''(p_m)]^{1/2}$, where Q'' is the second-order derivative of function Q, is a good approximation of the accelerated particles' flux level.

3. CONCLUSION AND DISCUSSION

With a prescribed finite shock thickness, diffusive compression acceleration automatically resolves the two limiting cases of particle acceleration. When the ratio of the upstream diffusion scale to the shock thickness, κ_1/V_1x_1, is greater than 1, the acceleration is very much like that due to a shock; otherwise, it behaves as adiabatic compressional acceleration. If the momentum dependence of the diffusion coefficient is known, we can also calculate the particle injection momentum and efficiency of shock acceleration. From the injection efficiency profile, we can establish the following criterion for shock acceleration:

$$\frac{\kappa_1}{V_1\Delta x_{sh}} > \frac{r}{r-1}. \quad (9)$$

This is the condition to judge whether a population of particles can be efficiently accelerated by a shock. Note that the momentum threshold for full injection efficiency may not necessarily be the momentum of particles actually injected to shock acceleration, because injection also depends on the spectrum of the source particles.

Our new shock injection criterion is different from those of Jokipii (1992), Webb et al. (1995), Zank et al. (2001), and Kallenbach et al. (2005), all of which are based on an argument by Jokipii (1987) that the particle gyroradius R_g is the lowest limit of the upstream diffusion scale, that is, $\kappa_1/V_1R_g > 1$. The criterion we set up here is less stringent than the previous ones because the shock thickness Δx_{sh} is independent of particle momentum, while R_g increases linearly with p. The shock thickness is generally on the order of the ion inertial length, that is, $\Delta x_{sh} = c/\omega_{pi}$, where c is the speed of light and ω_{pi} is the ion plasma oscillation frequency, which is proportional to the square root of the plasma density (see, e.g., Bale et al. 2003).

The diffusion coefficient normal to the shock comes from parallel diffusion $\kappa_\parallel$ and perpendicular diffusion $\kappa_\perp$ as $\kappa_1 = \kappa_{\parallel,1}\cos^2\theta + \kappa_{\perp,1}\sin^2\theta$, where θ is the angle of the upstream magnetic field to the shock normal; $\kappa_\perp$ is usually much smaller than $\kappa_\parallel$, as $\kappa_\parallel/\kappa_\perp = 1 + \eta_c^2$ with $\kappa_\parallel = \eta_c vR_g/3$ (Axford 1965). From the classical quasi-linear theory (Jokipii 1966), we take an η_c that is independent of particle momentum if the magnetic turbulence spectrum is of $1/f$ form. When $\tan\theta < (\kappa_{\parallel,1}/\kappa_{\perp,1})^{1/2}$, the acceleration is dominated by parallel diffusion. The threshold particle speed for injection with nearly full efficiency for a parallel shock is

$$v_i^{(\parallel)} > \sqrt{\frac{3crqBV_1}{(r-1)m\omega_{pi}\eta_c}} \quad \text{for} \quad \theta = 0^\circ, \quad (10)$$

where q and m are the charge and mass of the particles and B is the magnetic field strength. For a perpendicular shock with $\theta > \tan^{-1}(1 + \eta_c^2)^{1/2}$ (e.g., 81° for $\eta_c = 6$), which is probably rare due to the random walk of the field lines and the ruggedness of the shock surface, the injection threshold is

$$v_i^{(\perp)} > \sqrt{\frac{3crqBV_1(1+\eta_c^2)}{(r-1)m\omega_{pi}\eta_c}} \quad \text{for} \quad \theta = 90^\circ. \quad (11)$$

The injection threshold speed is inversely proportional to the mass-to-charge ratio, indicating preferential acceleration of heavier elements by shocks. Table 1 lists some typical values of the injection speed for a few types of shocks, where we have used $\eta_c = 6$ from Jokipii (1966). These numbers indicate that it is difficult to accelerate thermal particles, but pickup ions may be more readily available for shock acceleration. Only thermal particles having a decent fraction of the threshold injection speed may be accelerated, but with a low efficiency.

Finally, it should be pointed out that the approach to the shock injection problem presented in this paper can be viewed as a

parameterization approach within the framework of diffusion with a different geometry. It is meant to extrapolate the diffusive shock acceleration downward to see what is needed to limit particle injection at low energies. More precisely, it tries to establish a statistical requirement for particle transport when the particles just barely have enough energy to get back upstream of the shock. The diffusion coefficient should be related to the physics of wave-particle interaction (as in Malkov & Völk 1995), and the continuous shock profile needs to be related to the nonlinear modification of the shock by accelerated particles (similar to Malkov 1997; Blasi et al. 2005). It will be interesting to test this parameterization approach with numerical simulations.

I wish to thank Z. Saleh for helping me with MatLab. I also enjoyed useful discussions with H. Rassoul and C. Heredea. I am grateful to the Chinese Academy of Sciences for providing funding under National Natural Science Foundation grant 40621003. This work was supported in part by NASA under grants NAG 5-13514, NNG06G122G, and NNX07AH16G.

REFERENCES

Axford, W. I. 1965, Planet. Space Sci., 13, 115
Bale, S. D., Mozer, F. S., & Horbury, T. S. 2003, Phys. Rev. Lett., 91, No. 265004
Blasi, P., Gabici, S., & Vannoni, G. 2005, MNRAS, 361, 907
Drury, L. 1983, Space Sci. Rev., 36, 57
Drury, L. O'C., Axford, W. I., & Summers, D. 1982, MNRAS, 198, 833
Giacalone, J. 2005, ApJ, 628, L37
Giacalone, J., Jokipii, J. R., & Kóta, J. 2002, ApJ, 573, 845
Gloeckler, G., Geiss, J., & Fisk, L. A. 2001, in The Heliosphere near Solar Minimum, ed. A. Balogh, R. G. Marsden, & E. J. Smith (London: Springer), 287
Jokipii, J. R. 1966, ApJ, 146, 480
———. 1987, in Proc. 6th Int. Solar Wind Conf., ed. V. J. Pizzo, T. Holzer, & D. G. Sime (Boulder: Natl. Cent. Atmos. Res.), 481
———. 1992, ApJ, 393, L41
Kallenbach, R., Hilchenbach, M., Chalov, S. V., Le Roux, J. A., & Bamert, K. 2005, A&A, 439, 1
Lee, M. A., Shapiro, V. D., & Sagdeev, R. Z. 1996, J. Geophys. Res., 101, 4777
Malkov, M. A. 1997, ApJ, 491, 584
Malkov, M. A., & Völk, H. J. 1995, A&A, 300, 605
Scholer, M., & Kucharek, H. 1999, Geophys. Res. Lett., 26, 29
Scholer, M., et al. 1999, Space Sci. Rev., 89, 369
Webb, G. M., Zank, G. P., Ko, C. M., & Donohue, D. J. 1995, ApJ, 453, 178
Zank, G. P., Pauls, H. L., Cairns, I. H., & Webb, G. M. 1996, J. Geophys. Res., 101, 457
Zank, G. P., Rice, W. K. M., Le Roux, J. A., & Matthaeus, W. H. 2001, ApJ, 556, 494
Zhang, M. 2006, J. Geophys. Res., 111, No. A04208